Added mass of a disc accelerating within a pipe

J. D. Sherwood
Schlumberger Cambridge Research, High Cross, Madingley Road, Cambridge CB3 0EL, United Kingdom

H. A. Stone
Division of Engineering & Applied Sciences, Harvard University, Cambridge, Massachusetts 02138

(Received 1 April 1997; accepted 7 July 1997)

The flow of inviscid fluid around a disc in a pipe is computed, and the results are used to determine the added mass of the accelerating disc in the frame in which the mixture velocity is zero. The added mass of an array of discs spaced at regular intervals along the pipe is then computed, and is related to the pressure gradient along the pipe. Some flow profiles are also presented. The results show that the added mass per particle increases as the pipe diameter is reduced relative to the particle size. The added mass per particle decreases as the number density of particles increases, but the added mass per unit length of the pipe nevertheless increases. Thus an increase of either the particle size or number density leads to a tighter coupling between the liquid and the particles; this result should hold for other particle shapes and configurations. Results are also presented for the drift, i.e., the displacement of fluid particles caused by the motion of an isolated disc along the axis of the pipe. If the diameter of the pipe is sufficiently small, the added mass of the disc is modified from that in unbounded fluid, and the background drift at the walls of the pipe can no longer be estimated from the added mass of the disc. © *1997 American Institute of Physics.* [S1070-6631(97)02511-7]

I. INTRODUCTION

Models of two-phase flow require a constitutive relation for the forces which act between the liquid and gas. An approximation sometimes employed divides the forces into a sum of drag and added mass terms.[1–3] The added mass of a single spherical bubble in unbounded irrotational flow is well-known,[4] and results are available for the added mass of a spherical bubble in fluid which is accelerating.[4–6] The radius of the bubble need not be constant.[5] However, few results are available for the added mass of non-dilute suspensions, and fewer still treat flow in bounded geometries. We treat analytically an isolated disc accelerating in a pipe, as well as a regular array of accelerating discs, in order to obtain more insight into this problem.

A review of added mass in non-dilute suspensions is presented by Sangani *et al.*,[3] who are concerned with small amplitude oscillatory motion of bubbles. The average hydrodynamic force $\langle \boldsymbol{F} \rangle$ per bubble can be written in the form

$$\langle \boldsymbol{F} \rangle = \tfrac{1}{2} C_a \rho v_b \langle \dot{\boldsymbol{u}}_m - \dot{\boldsymbol{v}} \rangle + \rho v_b \langle \dot{\boldsymbol{u}}_m \rangle + 12\pi\mu R C_d \langle \boldsymbol{u}_m - \boldsymbol{v} \rangle, \tag{1}$$

where ρ and μ are the density and viscosity of the liquid, R and v_b are the radius and volume of the bubble, $\boldsymbol{u}_m$ is the mixture velocity, $\boldsymbol{v}$ is the bubble velocity, and $\langle . \rangle$ denotes an averaged quantity. The added mass coefficient C_a, and viscous drag coefficient C_d, have been normalized so that they approach unity as the volume fraction of bubbles $\beta \to 0$. Equation (1) can alternatively be written in terms of the average liquid velocity $\langle \boldsymbol{u} \rangle$ using the relation

$$\langle \boldsymbol{u}_m \rangle = (1-\beta)\langle \boldsymbol{u} \rangle + \beta \langle \boldsymbol{v} \rangle \tag{2}$$

if the volume fraction of bubbles, β, is assumed constant. From now on we neglect the viscous drag term, and set the viscosity $\mu = 0$.

Published results for the added mass coefficient C_a vary slightly, since some authors assume that all bubbles have the same velocity whereas others allow bubble velocities to vary. However, Sangani *et al.*[3,7] concluded that results of their numerical solutions of the full equations were closely approximated by the expression

$$C_a = \frac{1+2\beta}{1-\beta}, \tag{3}$$

obtained by Zuber[8] using a cell model. Ishii *et al.*[9] performed time-dependent computations of bubbly flows assuming an added mass $C_a = 1 + 2.78\beta$ due to Van Wijngaarden.[10] Thus there is a consensus of opinion that added mass increases as the volume fraction of liquid decreases (assuming that phase inversion does not occur). This increase can be thought of in terms of a tighter coupling between the dispersed particles and the liquid.

Many multiphase flows are confined to pipes, and only a few analytic results are available for such flows. Smythe computed the streamfunctions for inviscid irrotational flow in a pipe containing either a sphere[11] or a spheroid[12] (including the limiting case of a disc). Cai and Wallis[13,14] extended this analysis to linear arrays of spheres and obtained added mass coefficients; they also reported[14] the added mass of a single disc accelerating broadside in a pipe. We reconsider the case of a disc, using methods based on the velocity potential, and then study a linear array of discs in a pipe, working in a frame in which the average mixture velocity of the fluid and particles is zero. Acceleration of the particles leads to acceleration of the surrounding fluid, and this acceleration reaction, which corresponds to the added mass, creates pressure gradients. The net result is a macroscopic pressure gradient along the pipe. We find that the added mass coefficient C_a (per particle) increases as the particle size becomes closer to that of the pipe. As the particle number density increases,

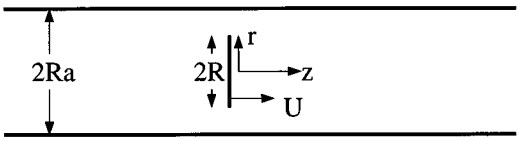

FIG. 1. A single disc, of radius R, on the centreline of a pipe of radius aR.

the added mass per particle decreases, because of shielding, but the added mass per unit length of pipe always increases.

As an additional application of the analysis, we calculate the drift of fluid markers disturbed by a steadily translating disc in a pipe. We are thus able to study the influence of the pipe walls on the typical magnitude of marker displacement.

II. ANALYSIS

We first consider the velocity potential for steady inviscid flow around a single disc of radius R moving broadside with velocity U along the axis of a pipe of radius Ra, as depicted in figure 1; results, calculated using a different method, have been reported by Cai and Wallis.[14] In Sec. III, we show how the added mass of an accelerating disc may be evaluated once the velocity potential is known, and numerical results are presented in Sec. IV. In Sec. V we consider a one-dimensional array of discs placed at regular intervals along the axis of the pipe. The discs have zero thickness, so that the volume fraction of discs within the pipe is always zero, even though the particle number density is non-zero. Nevertheless, a suspension of larger and more numerous discs ought to correspond physically to bubbly flows with increasing volume fraction of bubbles. Finally, fluid transport, studied via the concept of drift, is discussed for this bounded system in Sec. VI.

We assume an irrotational, incompressible flow, with velocity

$$\boldsymbol{u}=\nabla\phi, \tag{4}$$

where the potential ϕ satisfies Laplace's equation,

$$\nabla^2\phi=0. \tag{5}$$

Lengths are non-dimensionalized by R, and velocities by U. We use cylindrical coordinates, with $r=0$ as the axis of the pipe and the disc, and with the disc in the plane $z=0$. The boundary conditions, assuming no flow at infinity, are

$$u_z=\frac{\partial\phi}{\partial z}=1, \quad 0\leqslant r<1, \quad z=0, \tag{6a}$$

$$u_r=\frac{\partial\phi}{\partial r}=0, \quad 1\leqslant r\leqslant a, \quad z=0, \tag{6b}$$

$$u_r=\frac{\partial\phi}{\partial r}=0, \quad r=a, \quad \text{all } z, \tag{6c}$$

$$\nabla\phi\rightarrow\mathbf{0}, \quad z\rightarrow\pm\infty. \tag{6d}$$

We consider the region $z\geqslant 0$, and look for a solution of the form

$$\phi(r,z)=\sum_{n=1}^{\infty} b_n J_0(\lambda_n r)\exp(-\lambda_n z), \tag{7}$$

where the λ_n are chosen to satisfy

$$J_1(\lambda_n a)=0, \tag{8}$$

thereby ensuring that boundary condition (6c) is satisfied. Boundary conditions (6a,b) lead to

$$-1=\sum_{n=1}^{\infty} b_n\lambda_n J_0(\lambda_n r), \quad 0\leqslant r<1, \tag{9a}$$

$$0=\sum_{n=1}^{\infty} b_n\lambda_n J_1(\lambda_n r), \quad 1\leqslant r\leqslant a. \tag{9b}$$

In order to treat these dual series equations, we follow the method of Cooke and Tranter,[15] as described by Sneddon.[16] For completeness we present the most important intermediate results, beginning with the identity

$$\sum_{n=1}^{\infty}\frac{J_{\nu+2m+1-p}(\zeta_n)J_\nu(\zeta_n r)}{\zeta_n^{1-p}J_{\nu+1}^2(\zeta_n a)}=0, \quad 1<r\leqslant a, \tag{10}$$

where $-\frac{1}{2}\leqslant p\leqslant\frac{1}{2}$, $\nu>p-1$ and the ζ_n are the roots of $J_\nu(a\zeta_n)=0$. The boundary condition represented by (9b) may be satisfied if we take $\nu=1$ and

$$\lambda_n b_n=\sum_{m=0}^{\infty} c_m\frac{J_{2m+2-p}(\lambda_n)}{\lambda_n^{1-p}J_2^2(\lambda_n a)}, \tag{11}$$

i.e.,

$$b_n=[\lambda_n^{2-p}J_2^2(\lambda_n a)]^{-1}\sum_{m=0}^{\infty} c_m J_{2m+2-p}(\lambda_n). \tag{12}$$

An expression for the unknown c_m is obtained by substituting (11) into (9a):

$$-1=\sum_{n=1}^{\infty}\sum_{m=0}^{\infty}\frac{c_m J_{2m+2-p}(\lambda_n)J_0(\lambda_n r)}{\lambda_n^{1-p}J_2^2(\lambda_n a)}, \quad 0\leqslant r\leqslant 1. \tag{13}$$

Some relations concerning Bessel functions are now required in order to enable us to eliminate the r-dependence of (13). From Sneddon[16] (equations 2.1.19 and 2.1.20)

$$\int_0^\infty u^{1-k}J_{\nu+2m+k}(u)J_\nu(ru)\,\mathrm{d}u$$

$$=\frac{\Gamma(\nu+m+1)r^\nu(1-r^2)^{k-1}}{2^{k-1}\Gamma(\nu+1)\Gamma(m+k)}\mathscr{F}_m(k+\nu,\nu+1;r^2), \quad 0\leqslant r<1$$

$$=0, \quad r\geqslant 1, \tag{14}$$

where $\mathscr{F}_m(a,b;x)={}_2F_1(-m,a+m;b;x)$ is the Jacobi polynomial.

If we define the Hankel transform $\overline{f}(p)$ of $f(r)$ by

$$\overline{f}(p)=\int_0^\infty r f(r)J_n(pr)\,dr, \tag{15}$$

then the inverse transform is

$$f(r)=\int_0^\infty p\,\overline{f}(p)J_n(pr)dp, \tag{16}$$

and the Hankel inversion theorem applied to (14) gives

$$u^{-k}J_{\nu+2m+k}(u)=\int_0^1\frac{\Gamma(\nu+m+1)r^{1+\nu}(1-r^2)^{k-1}}{2^{k-1}\Gamma(\nu+1)\Gamma(m+k)}\times J_\nu(ru)\mathscr{F}_m(k+\nu,\nu+1;r^2)dr. \tag{17}$$

We also require the orthogonality relation for Jacobi polynomials (see, e.g., Magnus *et al.*[17]),

$$\int_0^1 r^{2\nu+1}(1-r^2)^{k-1}\mathscr{F}_n(k+\nu,\nu+1;r^2)dr=\frac{\Gamma(\nu+1)\Gamma(k)}{2\Gamma(\nu+k+1)}\delta_{0n}. \tag{18}$$

We now multiply both sides of (13) by $r(1-r^2)^{-p}\times\mathscr{F}_j(1-p,1;r^2)$ and integrate to obtain

$$-\frac{\Gamma(1-p)}{2\Gamma(2-p)}\delta_{0j}=\sum_{n=1}^\infty\sum_{m=0}^\infty\frac{c_mJ_{2m+2-p}(\lambda_n)J_{2j+1-p}(\lambda_n)\Gamma(j+1-p)}{2^p\Gamma(j+1)\lambda_n^{2-2p}J_2^2(\lambda_n a)}. \tag{19}$$

Hence the c_m satisfy the linear equations

$$-\frac{2^{p-1}\Gamma(j+1)\Gamma(1-p)}{\Gamma(2-p)\Gamma(j+1-p)}\delta_{0j}=\sum_{m=0}^\infty c_m\sum_{n=1}^\infty\frac{J_{2m+2-p}(\lambda_n)J_{2j+1-p}(\lambda_n)}{\lambda_n^{2-2p}J_2^2(\lambda_n a)}, \tag{20}$$

i.e.,

$$\sum_{m=0}^\infty A_{jm}c_m=B_j,\quad j=0,1,2,\ldots, \tag{21}$$

where

$$A_{jm}=\sum_{n=1}^\infty\frac{J_{2m+2-p}(\lambda_n)J_{2j+1-p}(\lambda_n)}{\lambda_n^{2-2p}J_2^2(\lambda_n a)} \tag{22}$$

and

$$B_j=-2^{p-1}/\Gamma(2-p),\quad j=0,$$
$$=0\quad\text{otherwise}. \tag{23}$$

The velocity potential $\phi(r,z)$ is constant over the plane $z=0$, $1\leqslant r\leqslant a$ external to the disc. We can evaluate this constant ϕ_0 at an individual point, but it is more convenient to take the average value

$$\phi_0=\frac{1}{\pi(a^2-1)}\int_1^a\phi(r,0)\,2\pi r\,dr=-\frac{2}{a^2-1}\sum_{n=1}^\infty\frac{b_nJ_1(\lambda_n)}{\lambda_n}, \tag{24}$$

and to work with the velocity potential

$$\Phi_z=\phi-\phi_0, \tag{25}$$

where the subscript z indicates that the potential corresponds to motion of the disc in the z direction. Note that $\Phi_z\to-\phi_0$ as $z\to\infty$, and $\Phi_z=0$ over the plane external to the disc. It is clear, by symmetry, that $\Phi_z(r,-z)=-\Phi_z(r,z)$.

III. ADDED MASS

The added mass of an object moving in unbounded fluid at rest at infinity is discussed by Batchelor.[4] We write the (dimensional) velocity potential $\tilde{\phi}$ in the form

$$\tilde{\phi}=R\boldsymbol{U}(t)\cdot\boldsymbol{\Phi}(\boldsymbol{x}-\boldsymbol{x}_0(t)), \tag{26}$$

where $\boldsymbol{x}_0(t)$ is the instantaneous position of the center of the body. In the absence of gravitational or other body forces, the unsteady form of Bernoulli's equation (equation 6.2.5 of Batchelor[4]) takes the form

$$\frac{\partial\tilde{\phi}}{\partial t}+\frac{\tilde{\boldsymbol{u}}^2}{2}+\frac{p}{\rho}=C, \tag{27}$$

where $\tilde{\boldsymbol{u}}$ is the (dimensional) fluid velocity, and C is a constant, independent of position, if the flow is irrotational.

Let S_1 be the surface of the body, with outward facing normal $\boldsymbol{n}$. Again following Batchelor[4] (p. 404), the hydrodynamic force $\boldsymbol{F}$ acting on the body in an inviscid flow is

$$\boldsymbol{F}=-\int_{S_1}p\boldsymbol{n}\,dS=\rho\int_{S_1}\left[\frac{\partial\tilde{\phi}}{\partial t}+\frac{\tilde{\boldsymbol{u}}^2}{2}\right]\boldsymbol{n}\,dS-\rho\int_{S_1}C\boldsymbol{n}\,dS \tag{28a}$$

$$=\rho R\int_{S_1}(\dot{\boldsymbol{U}}\cdot\boldsymbol{\Phi})\boldsymbol{n}\,dS+\rho\int_{S_1}[\tfrac{1}{2}\tilde{\boldsymbol{u}}^2-\boldsymbol{U}\cdot\tilde{\boldsymbol{u}}]\boldsymbol{n}\,dS, \tag{28b}$$

since in (28a) the integral of C over the surface of the body is zero. The second term on the right-hand side of (28b) corresponds to the force in steady motion, and $\boldsymbol{F}\cdot\boldsymbol{U}$ can be shown to be zero either for steady motion in unbounded fluid, or for motion parallel to the axis of a pipe. The first term in (28b) is the acceleration reaction, $\boldsymbol{G}$. In the absence of viscous effects $\boldsymbol{G}$ accounts for the total hydrodynamic force acting on the body as fluid surrounding the particle is accelerated. This acceleration reaction is often called the added mass of the particle.

If a disc of unit radius moves broadside with velocity U in unbounded fluid, the velocity potential is[18,19]

$$\tilde{\phi}(r,z)=\frac{2UR}{\pi}(z\,\cot^{-1}\lambda-\zeta)\quad(0\leqslant\zeta\leqslant1,\ 0\leqslant\lambda<\infty), \tag{29}$$

where the oblate spheroidal coordinates λ and ζ are defined by

$$z=\lambda\zeta,\quad r^2=(1+\lambda^2)(1-\zeta^2). \tag{30}$$

The region $\lambda=0$, $0\leqslant\zeta\leqslant1$ represents the surface $z=0^+$ of the disc, on which $\tilde{\phi}=-2UR(1-r^2)^{1/2}/\pi$. The reaction on a disc of radius R accelerating in the z direction is

$$G_z=-\frac{4\rho\dot{U}R^3}{\pi}\int_0^1(1-r^2)^{1/2}\,2\pi r\,dr=-\frac{8\rho\dot{U}R^3}{3}, \tag{31}$$

as obtained by Lamb[18] (p. 134).

If the disc accelerates in unbounded fluid, the pressure at infinity is uniform, but if the disc accelerates within a pipe, the pressures far upstream and far downstream of the disc differ. We assume that $p \to p_1$ as $z \to \infty$, and that $p \to p_2$ as $z \to -\infty$. Evaluating Bernoulli's equation (27) at $z = \pm\infty$ gives

$$\frac{p_1}{\rho} - R\dot{U}\phi_0 = \frac{p_2}{\rho} + R\dot{U}\phi_0, \tag{32}$$

and hence

$$R\dot{U}\phi_0 = \frac{p_1 - p_2}{2\rho}. \tag{33}$$

The acceleration reaction for the disc in a pipe is

$$G_z = 2\rho\dot{U}R^3 \int_0^1 \left[\sum_{n=1}^{\infty} b_n J_0(\lambda_n r) - \phi_0 \right] 2\pi r \, dr$$

$$= 4\pi\rho\dot{U}R^3 \left(\frac{a^2}{a^2-1} \right) \sum_{n=1}^{\infty} \frac{b_n J_1(\lambda_n)}{\lambda_n}, \tag{34}$$

and the jump in pressure between $z = \pm\infty$ is

$$p_1 - p_2 = 2\rho R\dot{U}\phi_0 = -\frac{4\rho R\dot{U}}{a^2-1} \sum_{n=1}^{\infty} \frac{b_n J_1(\lambda_n)}{\lambda_n}$$

$$= -\frac{G_z}{\pi a^2 R^2}. \tag{35}$$

Numerical results will be presented for the dimensionless reaction

$$\hat{G}_z = -G_z / \rho\dot{U}R^3. \tag{36}$$

The acceleration reaction G_z is in the opposite direction to the acceleration $\dot{U}$: the change in sign in (36) ensures that $\hat{G}_z > 0$.

Smythe[12] and Sangani *et al.*[3] discuss the relation between computations of added mass and of an analogous electrical conductivity problem. Suppose the pipe is filled with conducting fluid, so that, in the absence of a disc, the electrical potential is $\phi = VRz$. If an insulating disc of radius R is inserted at $z = 0$, and the total current remains unchanged, the electrical potential becomes

$$\phi = VRz - VR\Phi_z. \tag{37}$$

Hence the *additional* voltage drop ΔV between $z = \pm\infty$ due to the presence of the disc is

$$\Delta V = 2VR\phi_0, \tag{38}$$

which corresponds to the resistance of a fluid-filled pipe of length $2\phi_0 R$.

IV. NUMERICAL RESULTS

All Bessel functions were evaluated in double precision using the NAG routines S17DEF, S17AEF and S17AFF, and roots of (8) were obtained using part of a package of Bessel function integration routines.[20,21] Note that, for any given value of the argument z, the Bessel functions $J_\nu(z)$ become small for ν large. To avoid numerical underflow these functions are set to zero by S17DEF. The Γ function in (23) was evaluated by means of the NAG routine S14AAF. All the infinite sums are approximated by finite sums, so that (7) becomes

$$\phi(r,z) = \sum_{n=1}^{N} b_n J_0(\lambda_n r) \exp(-\lambda_n z), \tag{39}$$

where

$$b_n = [\lambda_n^{2-p} J_2^2(\lambda_n a)]^{-1} \sum_{m=0}^{M-1} c_m J_{2m+2-p}(\lambda_n),$$

$$n = 1, \ldots, N. \tag{40}$$

The c_m are obtained by solving the linear equations

$$\sum_{m=0}^{M-1} A_{jm} c_m = B_j, \quad j = 0, \ldots, J-1, \tag{41}$$

where

$$A_{jm} = \sum_{n=1}^{N} \frac{J_{2m+2-p}(\lambda_n) J_{2j+1-p}(\lambda_n)}{\lambda_n^{2-2p} J_2^2(\lambda_n a)}. \tag{42}$$

Equation (41) represents a set of J equations in M unknowns. In practice, if we fix N and take $M = J$, (41) may be solved only for sufficiently small M: the maximum M for which (41) may be solved by the NAG routine F04ATF depends upon the dimensionless pipe radius a. For the case $a = 5.0$, if we take $p = 0.5$ and $N = 1000$, then $\hat{G}_z = 2.79$ for $M = 112$ and the matrix A is ill-conditioned for larger values of M. If N is increased to 2000, the corresponding values are $M = 156$ and $\hat{G}_z = 2.73$, whereas at $N = 5000$, $M = 248$ and $\hat{G}_z = 2.70$. Results were similar for other values of p: $p = -0.5$, $N = 5000$ leads to $\hat{G}_z = 2.70$ for $M = 248$, with A ill-conditioned for $M > 255$.

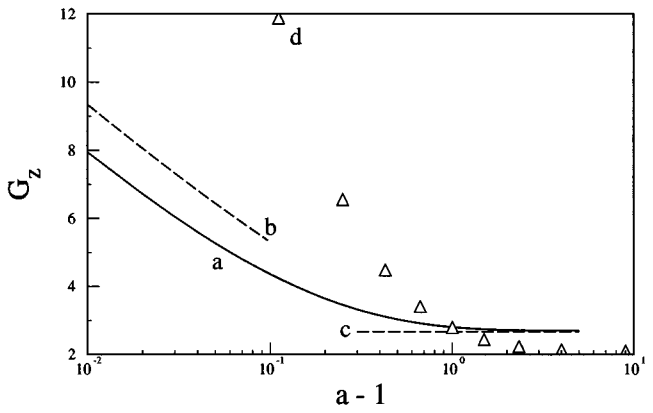

FIG. 2. The non-dimensional added mass coefficient $\hat{G}_z$ of a single disc in a pipe of radius a. (a) Numerical results; (b) asymptote (45) for $a - 1 \ll 1$, (c) limiting value $\hat{G}_z = 8/3$ for a disc in unbounded fluid, (d) $\triangle$ non-dimensional added mass of a single sphere in a pipe.[13]

Figure 2 shows values of $\hat{G}_z$ as a function of a, which agree with those of Cai and Wallis.[14] All results were computed with $N = 5000$, $p = 0.5$ and with M equal either to 300,

or to the maximum value for which equation (41) could be solved numerically. $\hat{G}_z$ decreases to 2.7 as a increases from 1 to 6. The numerical predictions then increase slowly as a increases further, rather than decreasing towards the value 8/3 predicted by (31). When $a=50$ the matrix A is ill-posed for $M>80$. Thus the numerical scheme becomes less satisfactory as a increases.

When $a-1\ll 1$, the flow into the narrow slit between the pipe and the edge of the disc may be approximated as that due to a line sink, restricted to an angle of $\pi/2$. The total (non-dimensional) volume flux due to the motion of the disc at unit velocity is π, and this flows into a slit of length $\pi(a+1)$, where we have taken the average of the inner and outer radii. Hence, close to the slit, the velocity potential has the form

$$\phi=\frac{2}{\pi(a+1)}\ln r_s, \tag{43}$$

where r_s is a radial coordinate local to the slit. If we assume that (43) holds from $r_s\sim a-1$ out to $r_s=1$, we might expect

$$\phi_0\sim\frac{2\ln(a-1)}{\pi(a+1)}, \tag{44}$$

and hence, by (35), the acceleration reaction should vary as

$$\hat{G}_z=2\pi a^2\phi_0\sim\frac{4a^2\ln(a-1)}{a+1}. \tag{45}$$

This asymptote (45) is shown in figure 2, and appears to be satisfactory. Quantitative agreement is improved if a constant 1.4 is subtracted from (45).

Also shown on figure 2 are results for the acceleration reaction on a sphere in a pipe, which was shown by Cai and Wallis[13] to be

$$G_z^{\text{sphere}}=\tfrac{4}{3}\pi R^3\rho\dot{U}(C_0^{\text{Smythe}}-1),$$

where C_0^{Smythe} is a coefficient computed by Smythe.[11,12] The acceleration reaction on a sphere in unbounded fluid is $2\pi R^3\rho\dot{U}/3$, and hence, with the non-dimensionalization (36) adopted here, $\hat{G}_z^{\text{sphere}}\to 2\pi/3$ as $a\to\infty$. The acceleration reaction on a sphere increases much more rapidly than that on a disc as the diameter of the pipe approaches that of the particle. In the case of a translating disc, rapid flow occurs only in a singular region around the edge of the disc. In the case of a sphere, rapid flow occurs along the entire length of the slowly varying narrow gap between the sphere and pipe.[13]

We may also compute the velocity field, given by

$$u_z(r,z)=-\sum_{n=1}^{\infty} b_n\lambda_n J_0(\lambda_n r)\exp(-\lambda_n z), \tag{46a}$$

$$u_r(r,z)=-\sum_{n=1}^{\infty} b_n\lambda_n J_1(\lambda_n r)\exp(-\lambda_n z). \tag{46b}$$

We might expect that (46a,b) should converge, for reasonable b_n, when $z>0$. However, convergence appears to be more problematic on $z=0$. In practice, computations of velocity are best performed for z slightly greater than 0, and

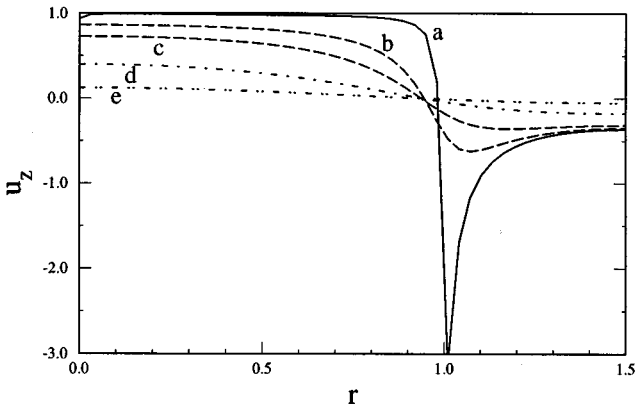

FIG. 3. The axial velocity profile u_z in a pipe of radius $a=1.5$ at positions $z=$ (a) 0.01, (b) 0.1, (c) 0.2, (d) 0.5, (e) 1.0.

$z\geqslant 0.01$ for the velocities presented here. Even so, results were poor on $r=0$, where we cannot rely on the decay of $J_0(\lambda_n r)$ as $\lambda_n\to\infty$. Figures 3 and 4 show profiles of $u_z(r)$ at various axial positions z. Near the edge of the disc the potential gradient $\nabla\phi$ has an $O(r_e^{-1/2})$ singularity, where r_e is a local cylindrical radial coordinate.[19] Hence it is not surprising that the numerical scheme has difficulty in resolving the velocity field in this region.

If the fluid velocity around a moving body is known, the viscous dissipation within the fluid may be computed, thereby giving an estimate of the viscous drag D on the body for cases in which viscous dissipation in boundary layers is small (such as clean bubbles). For example, if separation does not occur and flow is irrotational, the potential flow field may be used for such an estimate at high Reynold numbers. For a spherical bubble of radius R, moving at velocity U in unbounded fluid with viscosity μ, the drag is found[4] to be $D=12\pi\mu RU$. However, for the case considered here the velocity potential $\tilde{\phi}$ has an $O(r_e^{1/2})$ singularity at the edge of the disc: this can most easily be seen in the case of a disc moving in unbounded fluid (29). Rates of strain are $O(r_e^{-3/2})$, and hence the dissipation at the edge of the disc is

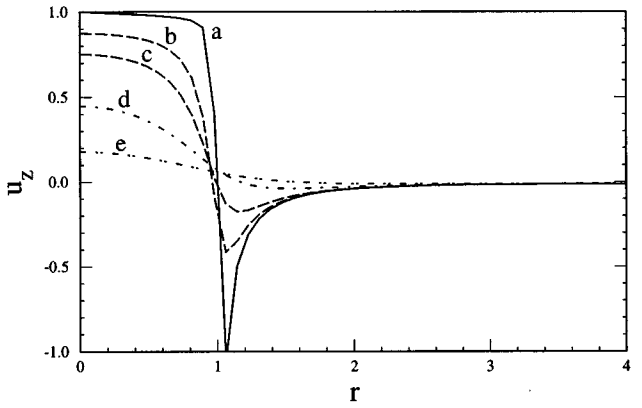

FIG. 4. The axial velocity profile u_z in a pipe of radius $a=4.0$ at positions $z=$ (a) 0.01, (b) 0.1, (c) 0.2, (d) 0.5, (e) 1.0.

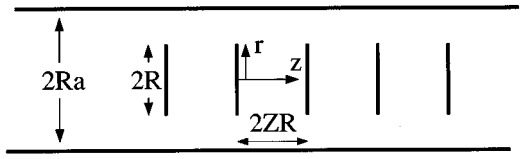

FIG. 5. An array of discs of radius R, spaced at intervals $2Z$ along the centreline of a pipe of radius aR.

not integrable. This serves as a reminder that in practice separation is likely to occur at the edge of the disc.

V. A LINEAR ARRAY OF DISCS

Suppose we have a regular array of discs, spaced with (non-dimensional) separation $2Z$ (figure 5). The radial velocity will be zero at the mid-point $z=Z$ between two such discs, and hence, instead of (7), we look for a velocity potential with the dimensionless form

$$\phi(r,z)=2\sum_{n=1}^{\infty} b_n J_0(\lambda_n r)\sinh[\lambda_n(Z-z)], \quad 0\leqslant z\leqslant Z. \tag{47}$$

We must still satisfy the boundary conditions (6a–c), and hence (9a,b) are replaced by

$$-1=2\sum_{n=1}^{\infty} b_n\lambda_n J_0(\lambda_n r)\cosh(\lambda_n Z), \quad 0\leqslant r<1, \tag{48a}$$

$$0=2\sum_{n=1}^{\infty} b_n\lambda_n J_1(\lambda_n r)\sinh(\lambda_n Z), \quad 1\leqslant r<a. \tag{48b}$$

In order to ensure that (48b) is satisfied identically, we take

$$2\lambda_n b_n\ \sinh(\lambda_n Z)=\sum_{m=0}^{\infty} c_m\frac{J_{2m+2-p}(\lambda_n)}{\lambda_n^{1-p}J_2^2(\lambda_n a)}. \tag{49}$$

Substituting (49) into (48a) we find that (13) is replaced by

$$-1=\sum_{n=1}^{\infty}\sum_{m=0}^{\infty}\frac{c_m J_{2m+2-p}(\lambda_n)J_0(\lambda_n r)\coth(\lambda_n Z)}{\lambda_n^{1-p}J_2^2(\lambda_n a)}, \quad 0\leqslant r\leqslant 1. \tag{50}$$

Hence, following the steps outlined in (14–19), we obtain the linear equations

$$\sum_{m=0}^{\infty} A_{jm}c_m=B_j, \quad j=0,1,2,\ldots, \tag{51}$$

where

$$A_{jm}=\sum_{n=1}^{\infty}\frac{J_{2m+2-p}(\lambda_n)J_{2j+1-p}(\lambda_n)\coth(\lambda_n Z)}{\lambda_n^{2-2p}J_2^2(\lambda_n a)}, \tag{52}$$

and the B_j are given by (23), as before. Note that (52) reduces to (22) in the limit $Z\to\infty$. The potential ϕ_0 over $r>1$ in the plane of the disc is evaluated, as in (24), by the integral

$$\phi_0=\frac{1}{\pi(a^2-1)}\int_1^a \phi(r,0)\ 2\pi r\ dr$$

$$=-\frac{4}{a^2-1}\sum_{n=1}^{\infty}\frac{b_n J_1(\lambda_n)}{\lambda_n}\sinh(\lambda_n Z), \tag{53}$$

and it is again convenient to work with the velocity potential

$$\Phi_z=\phi-\phi_0, \tag{54}$$

with $\Phi_z=0$ on $z=0$, and $\Phi_z=\mp\phi_0$ on $z=\pm Z$.

Note that the mean velocity over the pipe cross section is

$$\int_0^a 2\pi r u_z\ dr$$

$$=-\int_0^a 4\pi r\sum_{n=1}^{\infty}\lambda_n b_n J_0(\lambda_n r)\cosh[\lambda_n(Z-z)]dr$$

$$=4\pi a\sum_{n=1}^{\infty} b_n J_1(\lambda_n a)\cosh[\lambda_n(Z-z)]dr=0, \tag{55}$$

where we have used (8). Hence, as in Sec. II, we are in a frame in which the mean axial velocity of the liquid is zero. The discs have zero volume, and hence the mean axial velocity of the mixture is also zero.

Taking p_1 as the pressure at $z=Z$, and p_2 as the pressure at $z=-Z$, then evaluating Bernoulli's equation (27) at $z=\pm Z$, $r=0$, gives

$$C-\frac{\tilde{u}_z^2}{2}+U\tilde{u}_z=\frac{p_1}{\rho}-R\dot{U}\phi_0=\frac{p_2}{\rho}+R\dot{U}\phi_0, \tag{56}$$

where $\tilde{u}_z$ is the (dimensional) fluid velocity at $r=0$, $z=\pm Z$. Hence, as in (33),

$$R\dot{U}\phi_0=\frac{p_1-p_2}{2\rho}. \tag{57}$$

If the array of discs accelerates, the reaction on each disc is

$$G_z=2\rho\dot{U}R^3\int_0^1\left[\sum_{n=1}^{\infty} 2b_n J_0(\lambda_n r)\sinh(\lambda_n Z)-\phi_0\right]2\pi r\ dr$$

$$=8\pi\rho\dot{U}R^3\left(\frac{a^2}{a^2-1}\right)\sum_{n=1}^{\infty}\frac{b_n J_1(\lambda_n)\sinh(\lambda_n Z)}{\lambda_n}, \tag{58}$$

and the jump in pressure on $r=0$ between $z=\pm Z$ is

$$p_1-p_2=2\rho\dot{U}R\phi_0=-\frac{8\rho\dot{U}R}{a^2-1}\sum_{n=1}^{\infty}\frac{b_n J_1(\lambda_n)\sinh(\lambda_n Z)}{\lambda_n}$$

$$=-\frac{G_z}{\pi a^2R^2}. \tag{59}$$

Figure 6 shows the dimensionless acceleration reaction $\hat{G}_z=-G_z/\rho\dot{U}R^3$ as a function of disc separation Z, for the cases $a=1.1$, 1.5, 2.0 and 3.0. Note that $\hat{G}_z$ decreases as Z decreases, because the discs shield one another. Figure 7 shows similar results for the acceleration reaction per unit length $\hat{G}_z/2Z$, proportional to the pressure drop per unit length, which increases as Z decreases. Thus the liquid and discs become more tightly coupled, per unit length of pipe,

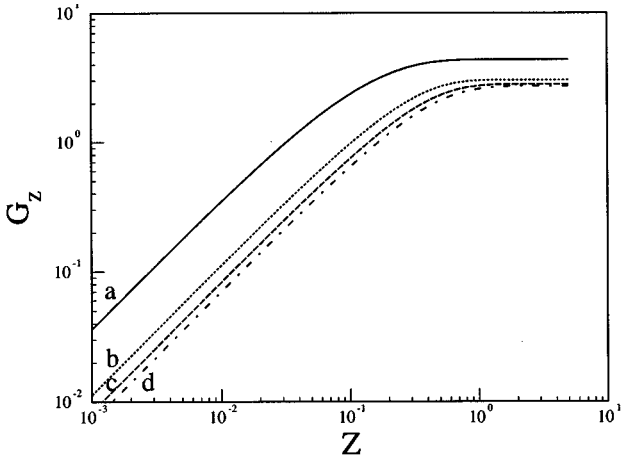

FIG. 6. The non-dimensional added mass coefficient $\hat{G}_z$, as a function of the disc separation $2Z$. Pipe radius $a=$ (a) 1.1, (b) 1.5, (c) 2.0, (d) 3.0.

when either the diameter of the discs increases relative to that of the pipe, or the number density of discs increases. We would expect this to be a general feature of suspensions of arbitrarily shaped particles.

When the discs are very close together, we might expect that the fluid between the discs in $r<1$ will, like the discs, have acceleration $\dot{U}$, and that the fluid in the annulus $r>1$ will have a mean acceleration $-\dot{U}/(a^2-1)$. We assume that the disc has no mass, so that the force required to accelerate the disc is equal and opposite to the acceleration reaction G_z. Equating the forces to mass accelerations in a unit cell $-Z\leqslant z\leqslant Z$, for the central core $r<1$,

$$2Z\pi\rho_l\dot{U}=-G_z-(p_1-p_2)\pi, \tag{60}$$

and for the outer annulus $1<r<a$,

$$-\frac{2Z\pi\rho_l\dot{U}}{a^2-1}=-(p_1-p_2)\pi. \tag{61}$$

Hence

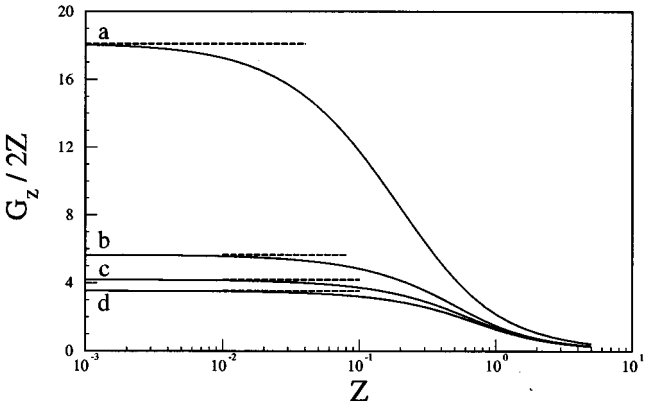

FIG. 7. As for figure 6, showing $\hat{G}_z/2Z$ as a function of Z. Broken lines indicate the limit $Z\to 0$ given by (62).

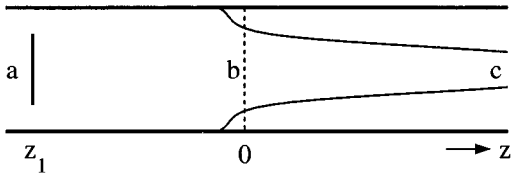

FIG. 8. Computation of drift. The disc (a) is shown in its initial position $z=z_1$; the broken line (b) shows the initial position of the marked fluid particles at $z=0$; line (c) shows the final position of the marked particles after the disc has moved off the figure to the right.

$$\frac{\hat{G}_z}{2Z}=\frac{\pi a^2}{a^2-1}. \tag{62}$$

The full numerical results agree well with (62) in the limit $Z\to 0$, as indicated in figure 7.

VI. DRIFT

If a particle of volume V moves along a pipe of cross-sectional area A filled with fluid at rest at infinity, the mean displacement of the fluid particles will be $-V/A$, as discussed by Eames *et al.*[22] and Benjamin.[23] However, the particle in some sense carries with itself a volume of liquid $R^3\hat{G}_z$ corresponding to the added mass of the particle; the background displacement of fluid, away from the wake of the particle, should therefore be $-(V+R^3\hat{G}_z)/A$. This line of argument has been used by Kowe *et al.*[24] to discuss the motion of bubbles relative to the interstitial fluid, and we examine these arguments for the case of a single disc moving in a tube.

We now change to coordinates fixed in space, rather than fixed in the disc (as previously). A line of marked fluid particles is placed at $z=0$. The motion of the fluid particles is followed while the disc moves from an initial position $z_1<0$ to a final position $z_2>0$: a marked fluid particle initially at $(r',0)$ eventually moves to (r,d) (see figure 8). Marked particles which are close to the axis of the pipe spend a

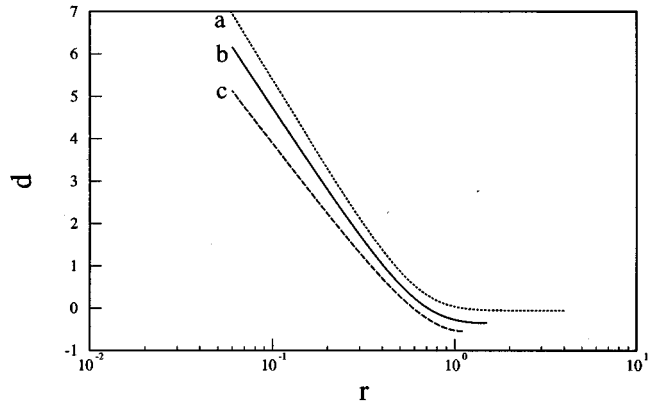

FIG. 9. The final positions of marked particles $z=d(r)$, initially on the plane $z=0$, after motion of a disc from $z=z_1=-\max(20,10a)$ to $z=z_2=-z_1$. The pipe radius is (a) $a=4.0$, (b) 1.5, (c) 1.1.

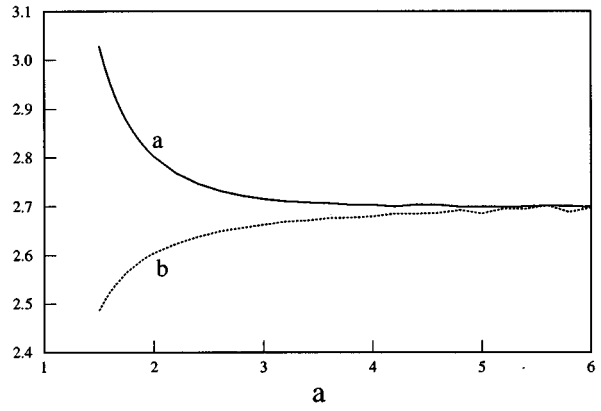

FIG. 10. (a) The non-dimensional added mass coefficient $\hat{G}_z$ of a single disc, as a function of pipe radius a. (b) The backwards background volume flux $-2\pi a^2 d(a)$ based on the wall drift $d(a)$.

considerable time in the vicinity of the stagnation points at the center of the front and rear faces of the disc. The displacement d of such particles is therefore large, with $d \sim \log(r)$, as discussed by Lighthill[25] for the case of drift around a spherical particle.

The initial and final positions of the disc were taken to be at $z = \pm \max(20, 10a)$, and in figure 9 we show the final displacements $d(r)$, for pipes with non-dimensional radius $a = 4$, 1.5 and 1.1. The average displacement $\int_0^a d(r) r \mathrm{d}r$ was computed: a numerical integration under the curves of figure 9 for $r > 0.06$ was cancelled, to within about 3% for $a < 3$, by an estimate of the integral of the logarithmic singularity in the region $r < 0.06$. This was a useful check on the accuracy of the integration of the trajectories of marked particles.

The disc has zero volume V, and hence when the pipe radius a is sufficiently large the background drift $-\pi a^2 d(a)$ should equal the non-dimensional added mass $\hat{G}_z$. In figure 10 we see that this is approximately true for $a > 5$: wall effects become important when $a < 5$.

ACKNOWLEDGMENT

This collaboration has been supported by the NATO Collaborative Research Grant Programme (CRG.961165).

[1] R. Clift, J. R. Grace, and M. E. Weber, *Bubbles, Drops and Particles* (Academic Press, New York, 1978).
[2] N. H. Thomas, T. R. Auton, K. Sene, and J. C. R. Hunt, ''Entrapment and transport of bubbles by transient large eddies in multiphase turbulent shear flow,'' in *International Conference on the Physical Modelling of Multiphase Flow, Coventry* (BHRA Fluid Engineering, Cranfield, England, 1983), p. 169.
[3] A. S. Sangani, D. Z. Zhang, and A. Prosperetti, ''The added mass, Basset, and viscous drag coefficients in non-dilute bubbly liquids undergoing small-amplitude oscillatory motion,'' Phys. Fluids A **3**, 2955 (1991).
[4] G. K. Batchelor, *An Introduction to Fluid Dynamics* (Cambridge University Press, Cambridge, 1973).
[5] D. Lhuillier, ''Forces d'inertie sur une bulle en expansion se déplaçant dans un fluide,'' Comptes Rend. Acad. Sci. Paris Sér II **295**, 95 (1982).
[6] T. R. Auton, J. C. R. Hunt, and M. Prud'homme, ''The force exerted on a body in inviscid unsteady non-uniform rotational flow,'' J. Fluid Mech. **197**, 241 (1988).
[7] A. S. Sangani and A. Prosperetti, ''Numerical simulation of the motion of particles at large Reynolds numbers,'' in *Particulate Two-Phase Flow*, edited by M. C. Roco (Butterworth-Heinemann, Boston, 1993), p. 971.
[8] N. Zuber, ''On the dispersed two-phase flow in the laminar-flow regime,'' Chem. Eng. Sci. **19**, 897 (1964).
[9] R. Ishii, Y. Umeda, and N. Shishido, ''Bubbly flows through a converging–diverging nozzle,'' Phys. Fluids A **5**, 1630 (1993).
[10] L. van Wijngaarden, ''Hydrodynamic interaction between gas bubbles,'' J. Fluid Mech. **77**, 27 (1976).
[11] W. R. Smythe, ''Flow around a sphere in a circular tube,'' Phys. Fluids **4**, 756 (1961).
[12] W. R. Smythe, ''Flow around a spheroid in a circular tube,'' Phys. Fluids **7**, 633 (1964).
[13] X. Cai and G. B. Wallis, ''Potential flow around a row of spheres in a circular tube,'' Phys. Fluids A **4**, 904 (1992).
[14] X. Cai and G. B. Wallis, ''The added mass coefficient for rows and arrays of spheres oscillating along the axes of tubes,'' Phys. Fluids A **5**, 1614 (1993).
[15] J. C. Cooke and C. J. Tranter, ''Dual Fourier–Bessel series,'' Q. J. Mech. Appl. Math. **12**, 379 (1959).
[16] I. N. Sneddon, *Mixed Boundary Value Problems in Potential Theory* (North-Holland, Amsterdam, 1966).
[17] W. Magnus, F. Oberhettinger, and R. P. Soni, *Formulas and Theorems for the Special Functions of Mathematical Physics* (Springer-Verlag, Berlin, 1966).
[18] H. Lamb, *Hydrodynamics*, 6th ed. (Cambridge University Press, Cambridge, England, 1932).
[19] J. D. Sherwood and H. A. Stone, ''Electrophoresis of a thin charged disc,'' Phys. Fluids **7**, 697 (1995).
[20] S. K. Lucas and H. A. Stone, ''Evaluating infinite integrals involving Bessel functions of arbitrary order,'' J. Comput. Appl. Math. **64**, 217 (1995).
[21] S. K. Lucas, ''Evaluating infinite integrals involving products of Bessel functions of arbitrary order,'' J. Comput. Appl. Math. **64**, 269 (1995).
[22] I. Eames, S. E. Belcher, and J. C. R. Hunt, ''Drift, partial drift and Darwin's proposition,'' J. Fluid Mech. **275**, 201 (1994).
[23] T. B. Benjamin, ''Note on added mass and drift,'' J. Fluid Mech. **169**, 251 (1986).
[24] R. Kowe, J. C. R. Hunt, A. Hunt, B. Couet, and L. J. S. Bradbury, ''The effects of bubbles on the volume fluxes and the pressure gradients in unsteady and non-uniform flow of liquids,'' Int. J. Multiphase Flow **14**, 587 (1988).
[25] M. J. Lighthill, ''Drift,'' J. Fluid Mech. **1**, 31 (1956).